

October 24, 2019



Clark Fork Bitterroot, Montana QL1 LiDAR Technical Data Report

Prepared For:



Steve Story

Montana Department of Natural Resources & Conservation
1424 9th Avenue
Helena, MT 59620
PH: 406-444-6816

Prepared By:



QSI Corvallis

1100 NE Circle Blvd, Ste. 126
Corvallis, OR 97330
PH: 541-752-1204

TABLE OF CONTENTS

INTRODUCTION	1
Deliverable Products	2
ACQUISITION	4
Planning.....	4
Boresight Calibration Flights.....	4
Airborne LiDAR Survey	5
Ground Survey.....	6
Base Stations.....	6
Ground Survey Points (GSPs).....	8
Land Cover Class	9
PROCESSING	11
LiDAR Data.....	11
Feature Extraction.....	13
Hydroflattening and Water’s Edge Breaklines.....	13
Contours	13
Buildings.....	14
RESULTS & DISCUSSION.....	15
LiDAR Density	15
LiDAR Accuracy Assessments	19
LiDAR Non-Vegetated Vertical Accuracy	19
LiDAR Vegetated Vertical Accuracies.....	22
LiDAR Relative Vertical Accuracy	23
LiDAR Horizontal Accuracy	24
CERTIFICATIONS	25
GLOSSARY	26
APPENDIX A - ACCURACY CONTROLS	27

Cover Photo: A view looking northeast over the Clark Fork river at Missoula, Montana. The image was derived from the LiDAR bare earth model and the above-ground point cloud and colored by elevation.

INTRODUCTION

This photo taken by QSI acquisition staff shows a scenic view of the Clark Fork Bitterroot project area in Clark County, Montana.



In February 2019, an amendment was made to the initial contract (WO-QSI-179) between Quantum Spatial, Inc. (QSI) and the State of Montana’s Department of Natural Resources and Conservation (MTDNRC), to collect Light Detection and Ranging (LiDAR) data in the spring of 2019 for expanded areas of interest over several counties in Montana, including: Powell and Deer Lodge Counties, Clark Fork River and Bitterroot River Corridors in Missoula and Granite Counties, additions to Hill and Valley Counties, and select tributary additions to Mineral County, Montana. All data were collected in support of MTDNRC’s objective of obtaining high resolution LiDAR-derived topographic data to aid in floodplain mapping being carried out by MTDNRC and the Federal Emergency Management Agency (FEMA).

This report accompanies the delivered LiDAR data for the Clark Fork Bitterroot LiDAR dataset, and documents contract specifications, data acquisition procedures, processing methods, and analysis of the final Clark Fork Bitterroot, Montana dataset including LiDAR accuracy and density. Acquisition dates and acreage are shown in Table 1, a complete list of contracted deliverables provided to MTDNRC is shown in Table 2, and the project extent is shown in Figure 1.

Table 1: Acquisition dates, acreage, and data types collected over the Clark Fork Bitterroot, Montana site

Project Site	Contracted Acres	Buffered Acres	Acquisition Dates	Data Type
Clark Fork Bitterroot, Montana	524,027	537,752	05/23/2019-06/16/2019	QL1 LiDAR
Clark Fork Bitterroot, Montana – Building Footprint AOI	153,890	169,883	05/23/2019-06/16/2019	QL1 LiDAR

Deliverable Products

Table 2: Products delivered to MTDNRC for the Clark Fork Bitterroot, Montana site

Clark Fork Bitterroot LiDAR Products Projection: Montana State Plane FIPS 2500 Horizontal Datum: NAD83 (2011) Vertical Datum: NAVD88 (GEOID12B) Horizontal Units: International Feet Units: US Survey Feet	
Points	LAS v 1.4 <ul style="list-style-type: none"> • Raw Calibrated Swaths • All Classified Returns
Rasters	Hydroflattened Bare Earth Digital Elevation Model (DEM): <ul style="list-style-type: none"> • 3.0 Foot Pixel Resolution • GeoTIFF Format • ESRI File Geodatabase Raster Dataset Format (*.gdb) • Space delimited ASCII Files (*.asc) Ground Density Raster Model: <ul style="list-style-type: none"> • 3.0 Foot Pixel Resolution • GeoTIFF Format Highest Hit Digital Surface Model (DSM): <ul style="list-style-type: none"> • 3.0 Foot Pixel Resolution • GeoTiff Format Intensity Images <ul style="list-style-type: none"> • 1.5 Foot Pixel Resolution • GeoTIFF Format
Vectors	Shapefiles (*.shp) <ul style="list-style-type: none"> • Site Boundary • Tile Index • Ground Survey Data • 1.0 Foot Contours • Total Area Flown • 3D Building Footprints • 3D Water's Edge Breaklines ESRI Geodatabase (*.gdb) <ul style="list-style-type: none"> • 1.0 Foot Contours • 3D Water's Edge Breaklines Space Delimited ASCII Text Files (*.txt) <ul style="list-style-type: none"> • 3D Water's Edge Breaklines

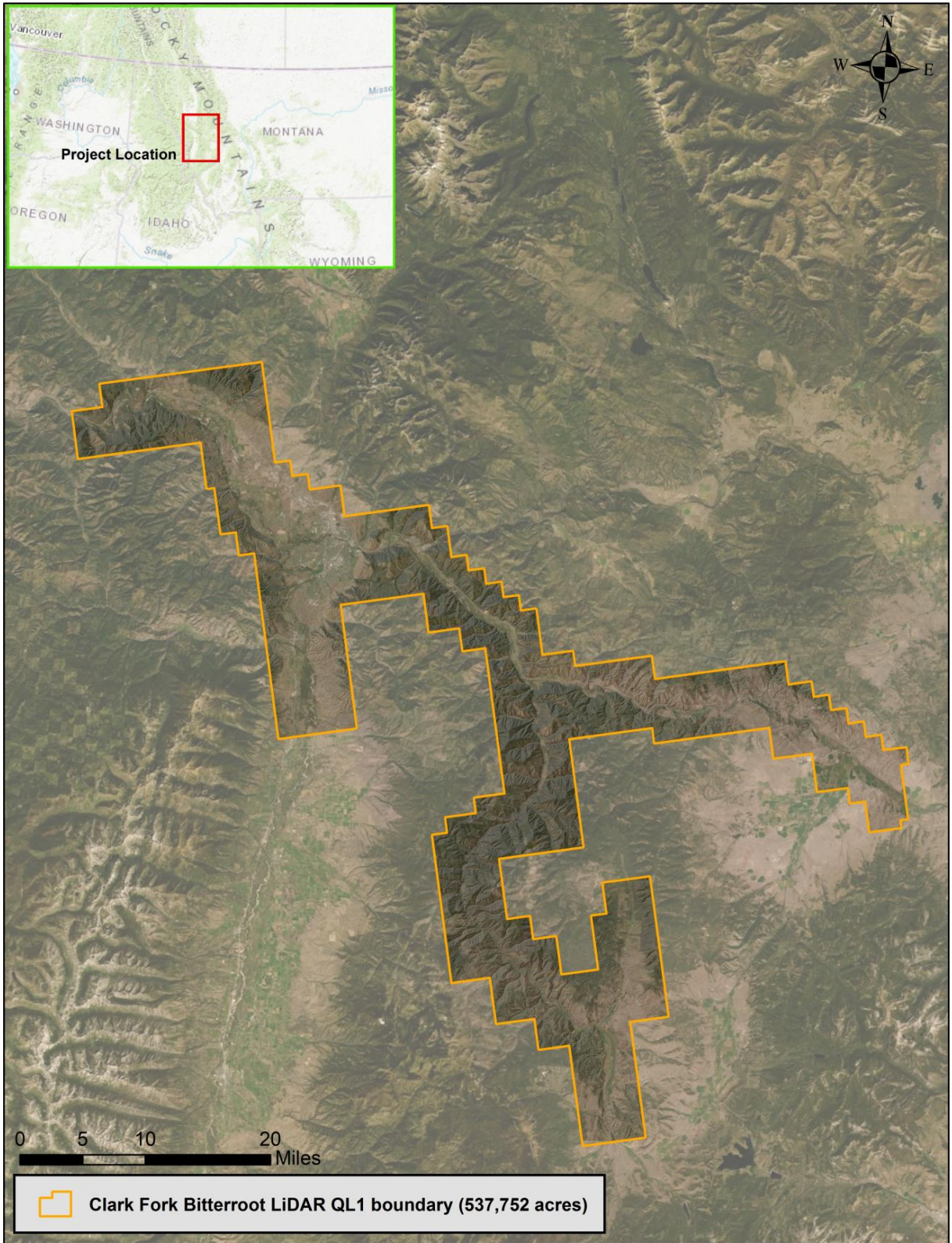


Figure 1: Location map of the Clark Fork Bitterroot, Montana site in Montana

Piper Navajo Aircraft, photo courtesy of airborneimagingusa.com



Planning

In preparation for data collection, QSI reviewed the project area and worked with Airborne Imaging, of Houston, Texas, to develop a specialized flight plan to ensure complete coverage of the Clark Fork Bitterroot, Montana QL1 LiDAR study area at the target point density of ≥ 8.0 points/m² (0.74 points/ft²). Acquisition parameters including orientation relative to terrain, flight altitude, pulse rate, scan angle, and ground speed were adapted to optimize flight paths and flight times while meeting all contract specifications.

Factors such as satellite constellation availability and weather windows must be considered during the planning stage. Any weather hazards or conditions affecting the flights were continuously monitored due to their potential impact on the daily success of airborne and ground operations. In addition, logistical considerations including private property access and potential air space restrictions were reviewed.

Boresight Calibration Flights

Prior to any data collection flights on a project, all aircraft and sensor pairings undergo a boresight calibration flight to ensure that installed equipment is functioning properly, and the lever arms are refined. In a boresight calibration flight, flight-lines are flown in a cross-hatch pattern to check for any inter- and intra-swath offsets or system misalignments. Additionally, QSI requires any acquisition subcontractor aircraft to undergo a boresight calibration flight prior to data collection in order to ensure data quality. Sensor and aircraft pairings and corresponding boresight requirements for the Clark Fork Bitterroot LiDAR data collection are detailed in Table 3 below.

Table 3: Boresight Calibration Flight Summary

LiDAR Boresight Calibration Flight Summary for Jefferson County, Montana Aircraft & Sensors				
Aircraft Name	Aircraft #	Sensor Name	Sensor Type	Boresight Flight Requirement
Piper Navajo	C-FVZM	SN2222738	Riegl VQ-1560i	Validated prior to flying on the project
Piper Navajo	C-FFRY	SN2223543	Riegl VQ-1560i	Validated prior to flying on the project
Piper Navajo	C-FKMA	SN2220754	Riegl Q-1560	Validated prior to flying on the project

Airborne LiDAR Survey

The LiDAR survey was accomplished using either a Riegl Q-1560 or VQ-1560i sensor system mounted in Airborne Imaging’s Piper Navajo aircraft. Table 4 summarizes the settings used to yield an average pulse density of ≥ 8 pulses/m² over the Clark Fork Bitterroot, Montana project area. The Riegl laser systems can record unlimited range measurements (returns) per pulse, however, it is not uncommon for some types of surfaces (e.g., dense vegetation or water) to return fewer pulses to the LiDAR sensor than the laser originally emitted. The discrepancy between first return and overall delivered density will vary depending on terrain, land cover, and the prevalence of water bodies. All discernible laser returns were processed for the output dataset.

Table 4: LiDAR specifications and survey settings

LiDAR Survey Settings & Specifications		
Acquisition Dates	05/23/19, 05/29/19	05/29/19, 05/30/19, 06/01/19 – 06/05/19, 6/12/19, 6/16/19
Aircraft Used	Piper Navajo (C-FKMA)	Piper Navajo (C-FVZM, C-FFRY)
Sensor	Riegl	Riegl
Laser	Q-1560	VQ-1560i
Maximum Returns	Unlimited	Unlimited
Resolution/Density	Average 8 pulses/m ²	Average 8 pulses/m ²
Nominal Pulse Spacing	0.35 m	0.35 m
Survey Altitude (AGL)	1800 m	1800 m
Survey speed	160 knots	160 knots
Field of View	60°	60°
Mirror Scan Rate	201 Hz	225 Hz
Target Pulse Rate	533.3 kHz	666.7 kHz
Pulse Length	3 ns	2.5 ns
Laser Pulse Footprint Diameter	32.4 cm	32.4 cm
Central Wavelength	1064 nm	1064 nm
Pulse Mode	Multi-Pulse in Air (MPiA)	Multi-Pulse in Air (MPiA)
Beam Divergence	0.18 mrad	0.18 mrad
Swath Width	2,078 m	2,078 m
Swath Overlap	67%	67%
Intensity	16-bit	16-bit
Accuracy	RMSE _z (Non-Vegetated) \leq 15 cm	RMSE _z (Non-Vegetated) \leq 15 cm
	NVA (95% Confidence Level) \leq 29.4 cm	NVA (95% Confidence Level) \leq 29.4 cm
	VVA (95 th Percentile) \leq 45 cm	VVA (95 th Percentile) \leq 45 cm

All areas were surveyed with an opposing flight line side-lap of $\geq 50\%$ ($\geq 100\%$ overlap) in order to reduce laser shadowing and increase surface laser painting. To accurately solve for laser point position (geographic coordinates x, y and z), the positional coordinates of the airborne sensor and the attitude of the aircraft were recorded continuously throughout the LiDAR data collection mission. Position of the aircraft was measured twice per second (2 Hz) by an onboard differential GPS unit, and aircraft attitude was measured 200 times per second (200 Hz) as pitch, roll and yaw (heading) from an onboard inertial measurement unit (IMU). To allow for post-processing correction and calibration, aircraft and sensor position and attitude data are indexed by GPS time.

Ground Survey

Ground control surveys, including monumentation and ground survey point (GSP) collection, were conducted by QSI to support the airborne acquisition. Ground control data were used to geospatially correct the aircraft positional coordinate data, and non-vegetated and vegetated check points were collected to perform quality assurance checks on final LiDAR data.



Base Stations

Base stations were utilized for collection of ground survey points using real time kinematic (RTK) survey techniques. RTK positioning is a relative-positioning method that improves the accuracy of GPS signals, which enhances the precision of location data obtained from satellite-based systems; because RTK positioning allows one to obtain centimeter-level positioning in real time, it remains the procedure of choice for applications that demand high-precision mapping.

Base Station locations were selected with consideration for satellite visibility, field crew safety, and optimal location for GSP coverage. Nine base stations in total were utilized for the Clark Fork Bitterroot LiDAR project. Seven of these base stations were monuments established by QSI, and the remaining two were permanent reference stations operated by the Montana State Reference Network (Table 5, Figure 2). New semi-permanent monumentation was set using 6" PK nail with a reference orange washer flagged with pink ribbon. QSI's professional land surveyor Steven J. Hyde (MTPLS#60192) oversaw and certified the establishment and utilization of all base stations utilized by QSI for the Clark Fork Bitterroot LiDAR Project.

Table 5: Monument positions for the Clark Fork Bitterroot, Montana acquisition. Coordinates are on the NAD83 (2011) datum, epoch 2010.00

Monument ID	Latitude	Longitude	Ellipsoid (meters)	Stability Rating	Owner
CLARK_BITTER_01	46° 54' 18.62095"	-114° 01' 56.53247"	968.224	D	QSI
DNRC19_RTK_06	46° 39' 34.70656"	-113° 09' 39.40169"	1221.242	D	QSI
DNRC19_RTK_07	46° 43' 27.49018"	-113° 34' 35.48070"	1090.334	D	QSI
DNRC19_RTK_08	46° 28' 44.00934"	-113° 46' 33.83044"	1290.227	D	QSI
DNRC19_RTK_09	46° 19' 46.47841"	-113° 32' 17.66480"	1483.807	D	QSI
DNRC19_RTK_10	46° 47' 39.42786"	-113° 44' 59.93279"	1032.18	D	QSI
DNRC19_RTK_11	47° 02' 02.84316"	-114° 20' 47.13101"	904.146	D	QSI
MSOL	46° 55' 45.83752"	-114° 06' 31.84467"	960.605	D	MTSRN
MTUM	46° 57' 00.08243"	-113° 28' 20.62252"	1122.762	D	MTSRN

QSI utilized static Global Navigation Satellite System (GNSS) data collected at 1 Hz recording frequency for each base station. During post-processing, the static GNSS data were triangulated with nearby Continuously Operating Reference Stations (CORS) using the Online Positioning User Service (OPUS¹) for precise positioning. Multiple independent sessions over the same monument were processed to confirm antenna height measurements and to refine position accuracy.

Monuments were established according to the national standard for geodetic control networks, as specified in the Federal Geographic Data Committee (FGDC) Geospatial Positioning Accuracy Standards for geodetic networks.² This standard provides guidelines for classification of monument quality at the 95% confidence interval as a basis for comparing the quality of one control network to another. The monument rating for this project is shown in Table 6.

Table 6: Federal Geographic Data Committee monument rating for network accuracy

Direction	Rating
1.96 * St Dev _{NE} :	0.020 m
1.96 * St Dev _z :	0.050 m

For the Clark Fork Bitterroot, Montana LiDAR project, the monument coordinates contributed no more than 5.4 cm of positional error to the geolocation of the final ground survey points and LiDAR, with 95% confidence.

¹ OPUS is a free service provided by the National Geodetic Survey to process corrected monument positions. <http://www.ngs.noaa.gov/OPUS>.

² Federal Geographic Data Committee, Geospatial Positioning Accuracy Standards (FGDC-STD-007.2-1998). Part 2: Standards for Geodetic Networks, Table 2.1, page 2-3. <http://www.fgdc.gov/standards/projects/FGDC-standards-projects/accuracy/part2/chapter2>

Ground Survey Points (GSPs)

Ground survey points were collected using real time kinematic (RTK), post-processed kinematic (PPK), and fast-static (FS) survey techniques. For RTK surveys, a roving receiver receives corrections from a nearby base station or Real-Time Network (RTN) via radio or cellular network, enabling rapid collection of points with relative errors less than 1.5 cm horizontal and 2.0 cm vertical. PPK and FS surveys compute these corrections during post-processing to achieve comparable accuracy. RTK and PPK surveys record data while stationary for at least five seconds, calculating the position using at least three one-second epochs. FS surveys record observations for up to fifteen minutes on each GSP in order to support longer baselines. All GSP measurements were made during periods with a Position Dilution of Precision (PDOP) of ≤ 3.0 with at least six satellites in view of the stationary and roving receivers. See Table 7 for Trimble unit specifications.

GSPs were collected in areas where good satellite visibility was achieved on paved roads and other hard surfaces such as gravel or packed dirt roads. GSP measurements were not taken on highly reflective surfaces such as center line stripes or lane markings on roads due to the increased noise seen in the laser returns over these surfaces. GSPs were collected within as many flightlines as possible; however, the distribution of GSPs depended on ground access constraints and monument locations and may not be equitably distributed throughout the study area (Figure 2).

Table 7: QSI ground survey equipment identification

Receiver Model	Antenna	OPUS Antenna ID	Use
Trimble R7 GNSS	Zephyr GNSS Geodetic Model 2 RoHS	TRM57971.00	Static, Rover



This photo taken by QSI acquisition staff shows a scenic view of the Clark Fork Bitterroot project area.

Land Cover Class

In addition to ground survey points, land cover class check points were collected throughout the study area to evaluate vertical accuracy. Vertical accuracy statistics were calculated for all land cover types to assess confidence in the LiDAR derived ground models across land cover classes (Table 8, see LiDAR Accuracy Assessments, page 19).

Table 8: Land Cover Types and Descriptions

Land cover type	Land cover code	Example	Description	Accuracy Assessment Type
Bare Earth	BE		Areas of bare earth surface	NVA
Forested	FR	 <small>Azimuth: 345° (N) Time: 09-20-2019 14:43:50 Note: FR003</small>	Areas dominated by coniferous or deciduous trees	VVA
Shrubs	SH		Areas dominated by herbaceous shrubland	VVA
Tall Grass	TG	 <small>Azimuth: 322° (NW) Time: 09-20-2019 15:38:25 Note: TG004</small>	Unmaintained grassland or grassland in advanced growth stage	VVA
Urban	URBAN		Areas dominated by urban development, including parks	NVA

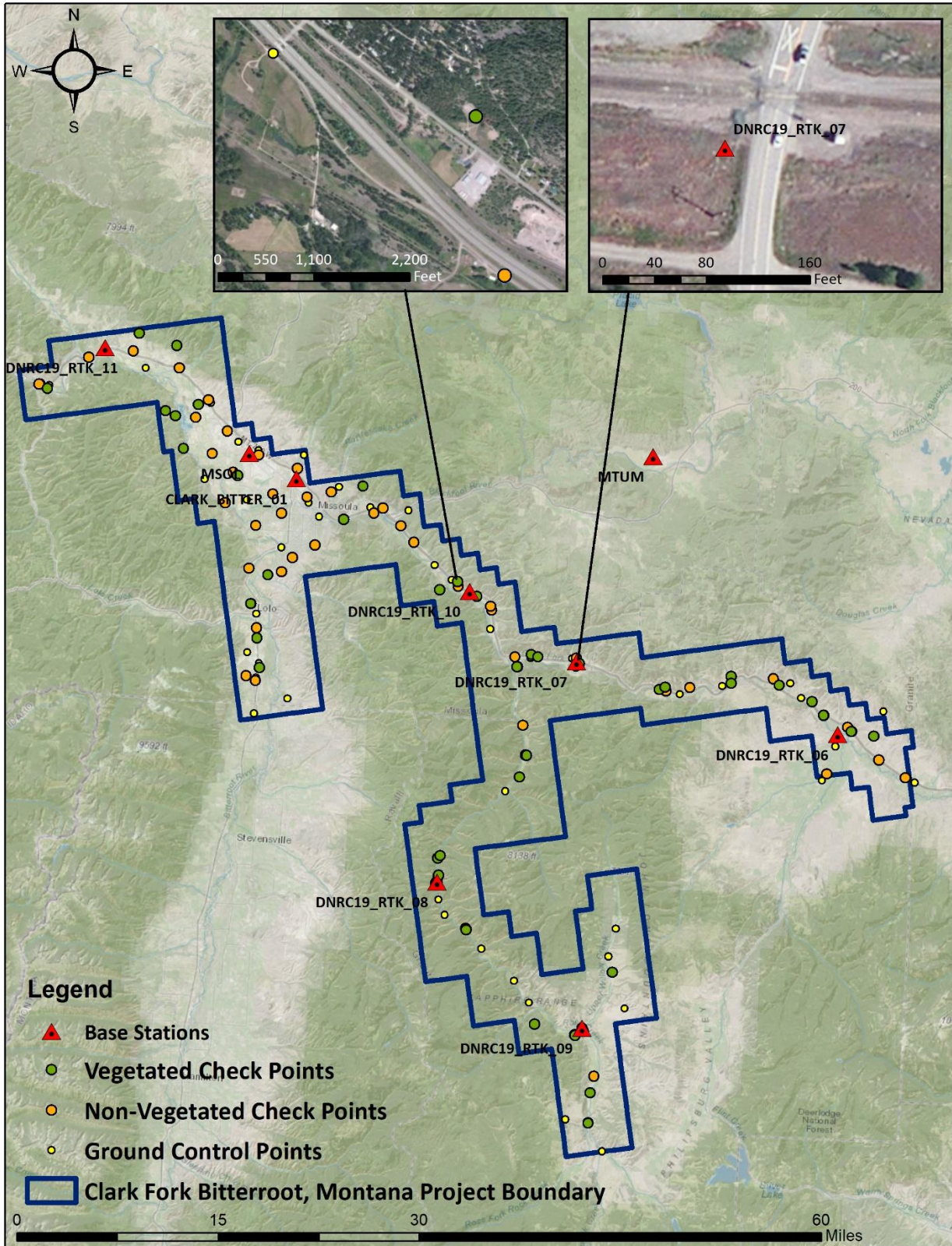


Figure 2: Ground survey location map

PROCESSING

- Default
- Ground
- Building
- Water

This 2 meter LiDAR cross section shows a view of the Clark Fork Bitterroot landscape, colored by point classification.



LiDAR Data

Upon completion of data acquisition, QSI processing staff initiated a suite of automated and manual techniques to process the data into the requested deliverables. Processing tasks included GPS control computations, smoothed best estimate trajectory (SBET) calculations, kinematic corrections, calculation of laser point position, sensor and data calibration for optimal relative and absolute accuracy, and LiDAR point classification (Table 9). Processing methodologies were tailored for the landscape. Brief descriptions of these tasks are shown in Table 10. Outlier points in the classified point cloud data are classified as Noise (Class 7) and make up approximately 1.80% of the delivered classified point cloud.

Table 9: ASPRS LAS classification standards applied to the Clark Fork Bitterroot, Montana dataset

Classification Number	Classification Name	Classification Description
1	Default/Unclassified	Laser returns that are not included in the ground class, composed of vegetation and anthropogenic features
1-0	Overlap/Edge Clip	Flightline edge clip, identified using the overlap flag
2	Ground	Laser returns that are determined to be ground using automated and manual cleaning algorithms
6	Buildings	Permanent building structures with minimum area 100ft ² or larger, classified using automated routines.
7	Noise	Laser returns that are often associated with birds, scattering from reflective surfaces, or artificial points below the ground surface
9	Water	Laser returns that are determined to be water using automated and manual cleaning algorithms
17	Bridge	Bridge deck
20	Ignored Ground	Ground points proximate to water's edge breaklines; ignored for correct model creation

Table 10: LiDAR processing workflow

LiDAR Processing Step	Software Used
Resolve kinematic corrections for aircraft position data using kinematic aircraft GPS and static ground GPS data. Develop a smoothed best estimate of trajectory (SBET) file that blends post-processed aircraft position with sensor head position and attitude recorded throughout the survey.	POSPac MMS v.8.2
Calculate laser point position by associating SBET position to each laser point return time, scan angle, intensity, etc. Create raw laser point cloud data for the entire survey in *.las (ASPRS v. 1.4) format. Convert data to orthometric elevations by applying a geoid correction.	POSPac MMS v.8.2 RiProcess v1.8.5
Import raw laser points into manageable blocks to perform manual relative accuracy calibration and filter erroneous points. Classify ground points for individual flight lines.	TerraScan v.19
Using ground classified points per each flight line, test the relative accuracy. Perform automated line-to-line calibrations for system attitude parameters (pitch, roll, heading), mirror flex (scale) and GPS/IMU drift. Calculate calibrations on ground classified points from paired flight lines and apply results to all points in a flight line. Use every flight line for relative accuracy calibration.	TerraMatch v.19
Classify resulting data to ground and other client designated ASPRS classifications (Table 9). Assess statistical absolute accuracy via direct comparisons of ground classified points to ground control survey data.	TerraScan v.19 TerraModeler v.19
Generate bare earth models as triangulated surfaces, and highest hit models as a surface expression of all points. Export surface models as GeoTiffs at a 3.0-foot pixel resolution. Duplicate in .gdb and .asc format.	TerraScan v.19 TerraModeler v.19 ArcMap v. 10.3.1
Export intensity images as GeoTIFFs at a 1.5-foot pixel resolution.	LAS Product Creator 3.0 (QSI proprietary) ArcMap v. 10.3.1
Generate contour lines from classified contour keypoints. Export all contours as polyline shapefiles. Generate final building footprint from classified LiDAR point cloud.	TerraScan v.19 TerraModeler v.19 ArcMap v. 10.3.1

Feature Extraction

Hydroflattening and Water's Edge Breaklines

The Clark Fork River and Bitterroot River, and other water bodies within the project area were flattened to a consistent water level. Bodies of water that were flattened include lakes and other closed water bodies with a surface area greater than 2 acres, all streams and rivers that are nominally wider than 30 meters, all non-tidal waters bordering the project, and select smaller bodies of water as feasible. The hydroflattening process eliminates artifacts in the digital terrain model caused by both increased variability in ranges or dropouts in laser returns due to the low reflectivity of water.

Hydroflattening of closed water bodies was performed through a combination of automated and manual detection and adjustment techniques designed to identify water boundaries and water levels. Boundary polygons were developed using an algorithm which weights LiDAR-derived slopes, intensities, and return densities to detect the water's edge. The water edges were then manually reviewed and edited as necessary. Specific care was taken to not hydroflatten wetland and marsh habitat found throughout the study site.

Once polygons were developed the initial ground classified points falling within water polygons were reclassified as water points to omit them from the final ground model. Elevations were then obtained from the filtered LiDAR returns to create the final breaklines. Lakes were assigned a consistent elevation for an entire polygon while rivers were assigned consistent elevations on opposing banks and smoothed to ensure downstream flow through the entire river channel.

Water boundary breaklines were then incorporated into the hydroflattened DEM by enforcing triangle edges (adjacent to the breakline) to the elevation values of the breakline. This implementation corrected interpolation along the hard edge. Water surfaces were obtained from a TIN of the 3-D water edge breaklines resulting in the final hydroflattened model.

Contours

Contour generation from LiDAR point data required a thinning operation in order to reduce contour sinuosity. The thinning operation reduced point density where topographic change is minimal (i.e., flat surfaces) while preserving resolution where topographic change was present. Contours were produced through TerraModeler by interpolating between contour key points at even elevation increments. Contours were generated at a 1 foot interval for the Clark Fork Bitterroot LiDAR dataset, with major contours labeled at 10 foot increments.

Areas averaging less than 0.05 ground-classified points per square foot were considered low confidence in the elevation data and correspond with the low confidence polygon shapefile called `S_Topo_Confidence`. Areas with low ground point density are commonly beneath buildings and bridges, in locations with dense vegetation, over water, and in other areas where the LiDAR is unable to sufficiently penetrate to the ground surface.

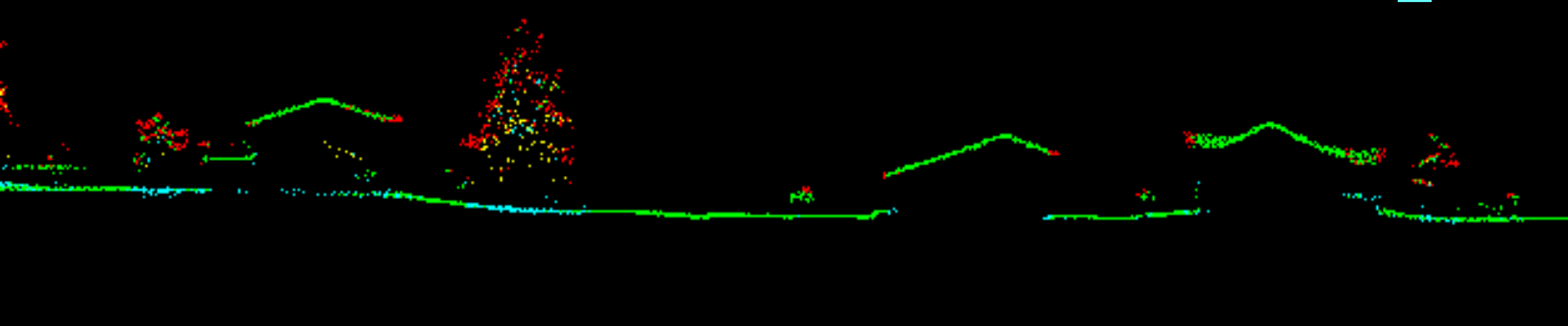
Buildings

Building classification was performed through a combination of automated algorithms and manual classification. Typically, manual editing of the building classification was necessary where dense canopy was immediately proximate to features. All non-mobile structures such as houses, barns, silos and sheds, with a minimum mapping size of $\geq 100\text{ft}^2$, were classified into the building category. Once classification was complete, automated routines were used to generate the polygon shapefile representing building footprints. Features were reviewed and manually edited as necessary, and each polygon was attributed with average height and lowest adjacent grade (LAG) fields. A total of 58,747 buildings were classed in the data (Figure 3).



Figure 3: Example of building footprint feature extraction, created from the Clark Fork Bitterroot above-ground LiDAR point cloud colored by intensity, overlaid with the 3D building polygon

This LiDAR cross section shows a view of vegetation, buildings, and bare ground in the Clark Fork Bitterroot AOI, colored by point laser echo.



LiDAR Density

The acquisition parameters were designed to acquire an average first-return density of 8 points/m² (0.74 points/ft²). First return density describes the density of pulses emitted from the laser that return at least one echo to the system. Multiple returns from a single pulse were not considered in first return density analysis. Some types of surfaces (e.g., breaks in terrain, water and steep slopes) may have returned fewer pulses than originally emitted by the laser. First returns typically reflect off the highest feature on the landscape within the footprint of the pulse. In forested or urban areas the highest feature could be a tree, building or power line, while in areas of unobstructed ground, the first return will be the only echo and represents the bare earth surface.

The density of ground-classified LiDAR returns was also analyzed for this project. Terrain character, land cover, and ground surface reflectivity all influenced the density of ground surface returns. In vegetated areas, fewer pulses may penetrate the canopy, resulting in lower ground density.

The average first-return density of LiDAR data for the Clark Fork Bitterroot, Montana project was 1.21 points/ft² (12.98 points/m²) while the average ground classified density was 0.33 points/ft² (3.52 points/m²) (Table 11). The statistical and spatial distributions of first return densities and classified ground return densities per 100 m x 100 m cell are portrayed in Figure 4 through Figure 7.

Table 11: Average LiDAR point densities

Classification	Point Density
First-Return	1.21 points/ft ²
	12.98 points/m ²
Ground Classified	0.33 points/ft ²
	3.52 points/m ²

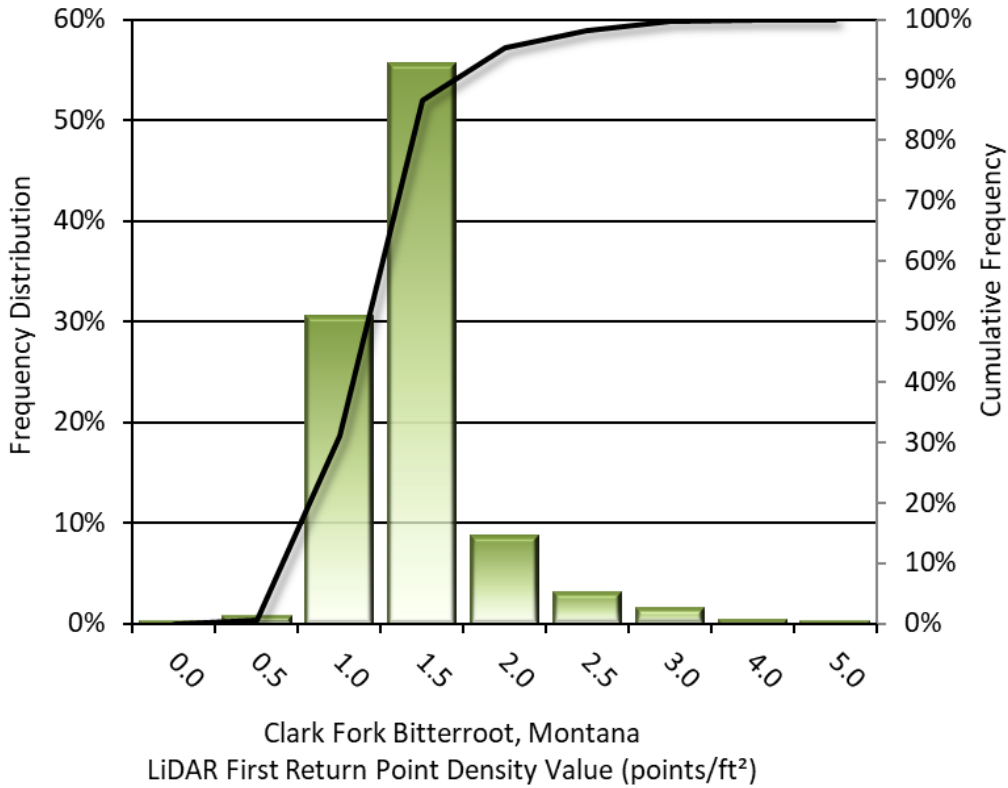


Figure 4: Frequency distribution of first return point density values per 100 x 100 m cell

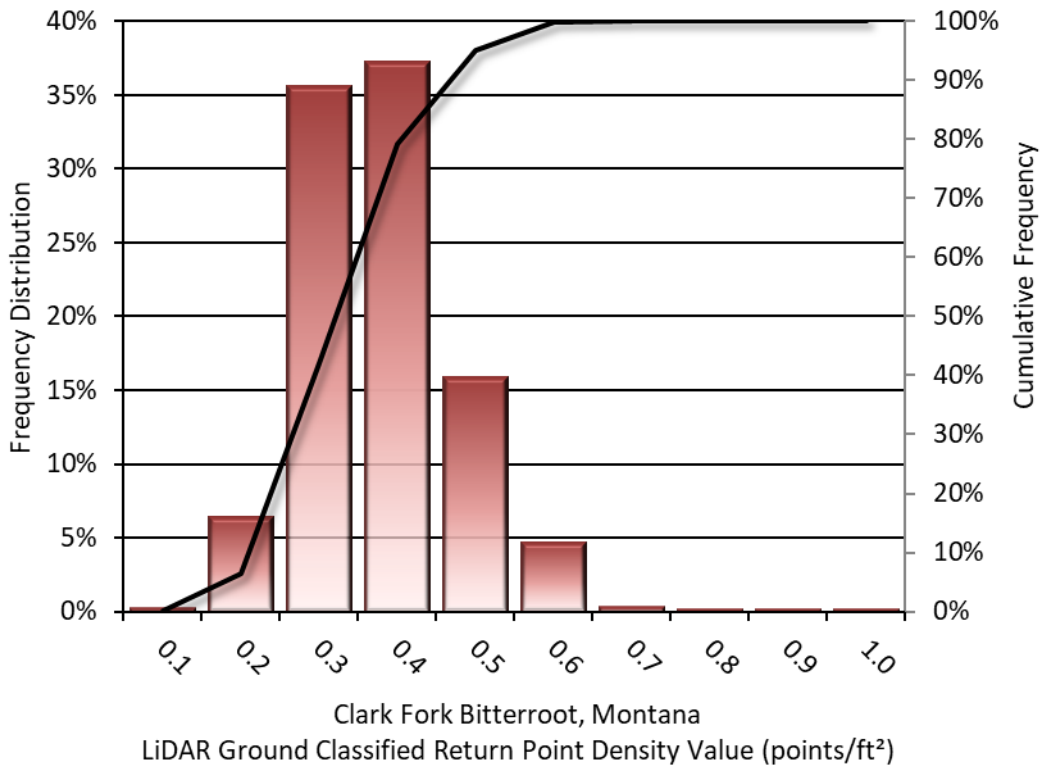


Figure 5: Frequency distribution of ground-classified return point density values per 100 x 100 m cell

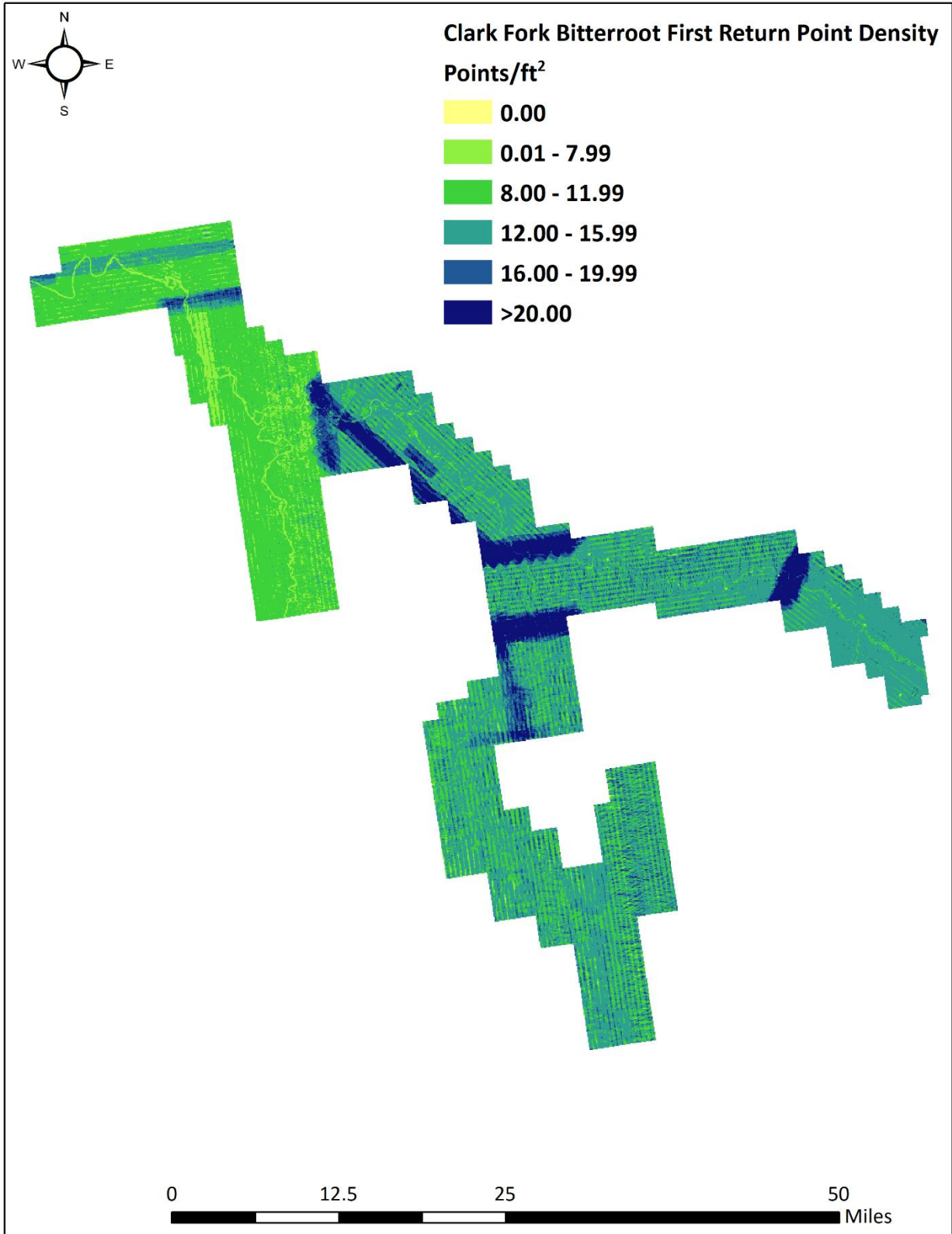


Figure 6: First return and ground-classified point density map for the Clark Fork Bitterroot, Montana site (100 m x 100 m cells)

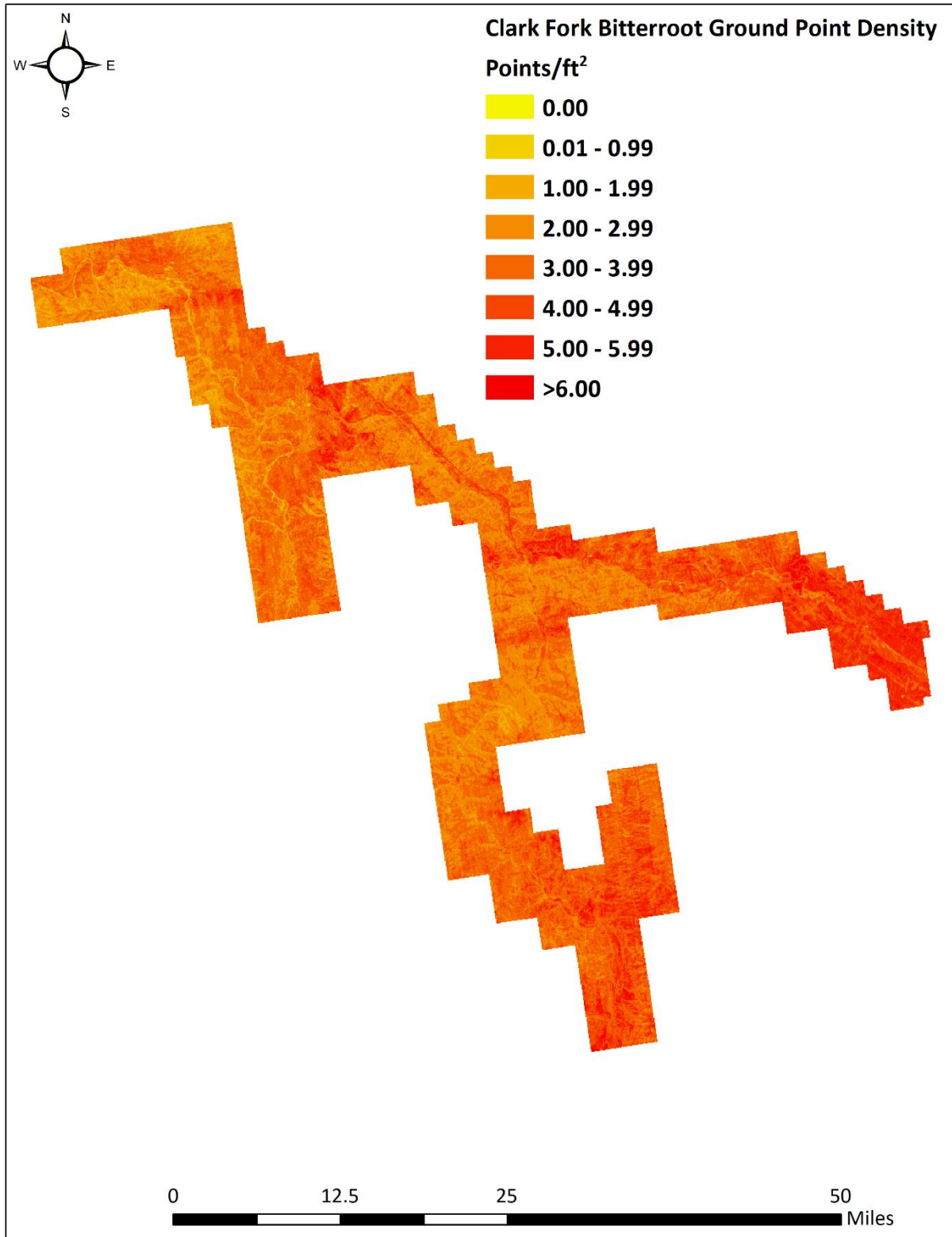


Figure 7: Ground-classified point density map for the Clark Fork Bitterroot, Montana site (100 m x 100 m cells)

LiDAR Accuracy Assessments

The accuracy of the LiDAR data collection can be described in terms of absolute accuracy (the consistency of the data with external data sources) and relative accuracy (the consistency of the dataset with itself). See Appendix A for further information on sources of error and operational measures used to improve relative accuracy.

LiDAR Non-Vegetated Vertical Accuracy

Absolute accuracy was assessed using Non-Vegetated Vertical Accuracy (NVA) reporting designed to meet guidelines presented in the FGDC National Standard for Spatial Data Accuracy³. NVA compares known ground check point data that were withheld from the calibration and post-processing of the LiDAR point cloud to the triangulated surface generated by the unclassified LiDAR point cloud as well as the derived gridded bare earth DEM. NVA is a measure of the accuracy of LiDAR point data in open areas where the LiDAR system has a high probability of measuring the ground surface and is evaluated at the 95% confidence interval ($1.96 * RMSE$), as shown in Table 12.

The mean and standard deviation (sigma σ) of divergence of the ground surface model from quality assurance point coordinates are also considered during accuracy assessment. These statistics assume the error for x, y and z is normally distributed, and therefore the skew and kurtosis of distributions are also considered when evaluating error statistics. For the Clark Fork Bitterroot, Montana survey, 55 ground check points were withheld from the calibration and post processing of the LiDAR point cloud, with resulting non-vegetated vertical accuracy of 0.169 feet (0.051 meters) as compared to unclassified LAS, and 0.210 feet (0.064 meters) as compared to the bare earth DEM, with 95% confidence (Figure 8, Figure 9).

QSI also assessed absolute accuracy using 61 ground control points. Although these points were used in the calibration and post-processing of the LiDAR point cloud, they still provide a good indication of the overall accuracy of the LiDAR dataset, and therefore have been provided in Table 12 and Figure 10.

³ Federal Geographic Data Committee, ASPRS POSITIONAL ACCURACY STANDARDS FOR DIGITAL GEOSPATIAL DATA EDITION 1, Version 1.0, NOVEMBER 2014. <http://www.asprs.org/PAD-Division/ASPRS-POSITIONAL-ACCURACY-STANDARDS-FOR-DIGITAL-GEOSPATIAL-DATA.html>.

Table 12: Absolute accuracy results

Absolute Vertical Accuracy			
	NVA, as compared to unclassified LAS	NVA, as compared to bare earth DEM	Ground Control Points
Sample	55 points	55 points	61 points
95% Confidence (1.96*RMSE)	0.169 ft 0.051 m	0.210 ft 0.064 m	0.209 ft 0.064 m
Average	0.029 ft 0.009 m	-0.044 ft -0.013 m	-0.039 ft -0.012 m
Median	0.033 ft 0.010 m	-0.033 ft -0.010 m	-0.030 ft -0.009 m
RMSE	0.086 ft 0.026 m	0.107 ft 0.033 m	0.107 ft 0.033 m
Standard Deviation (1σ)	0.082 ft 0.025 m	0.099 ft 0.030 m	0.100 ft 0.031 m

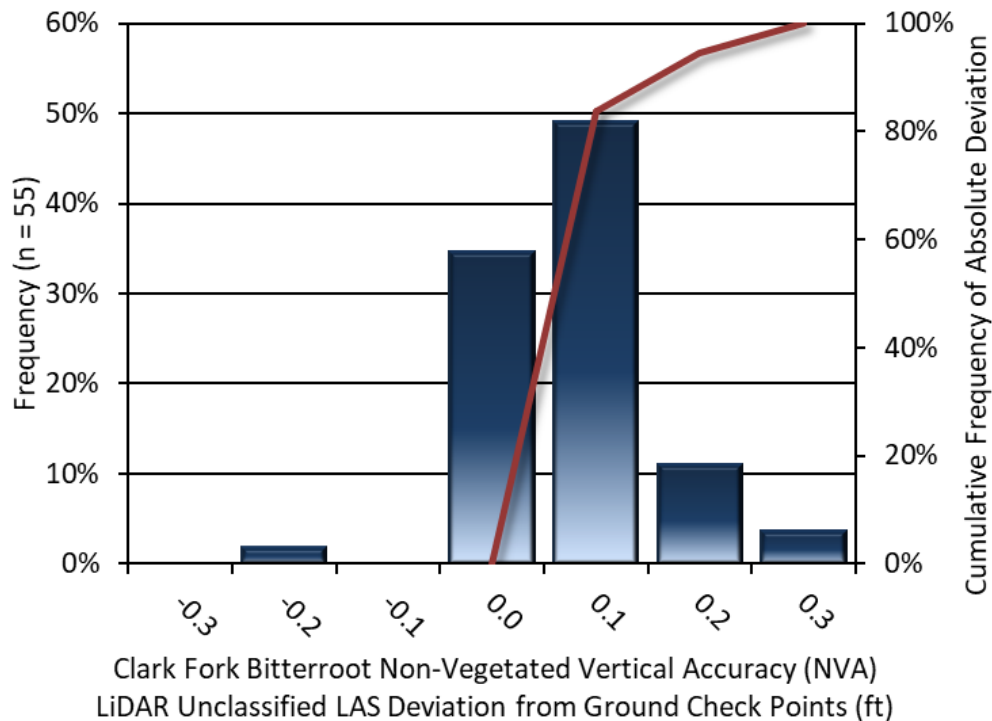


Figure 8: Frequency histogram for LiDAR unclassified LAS deviation from ground check point values (NVA)

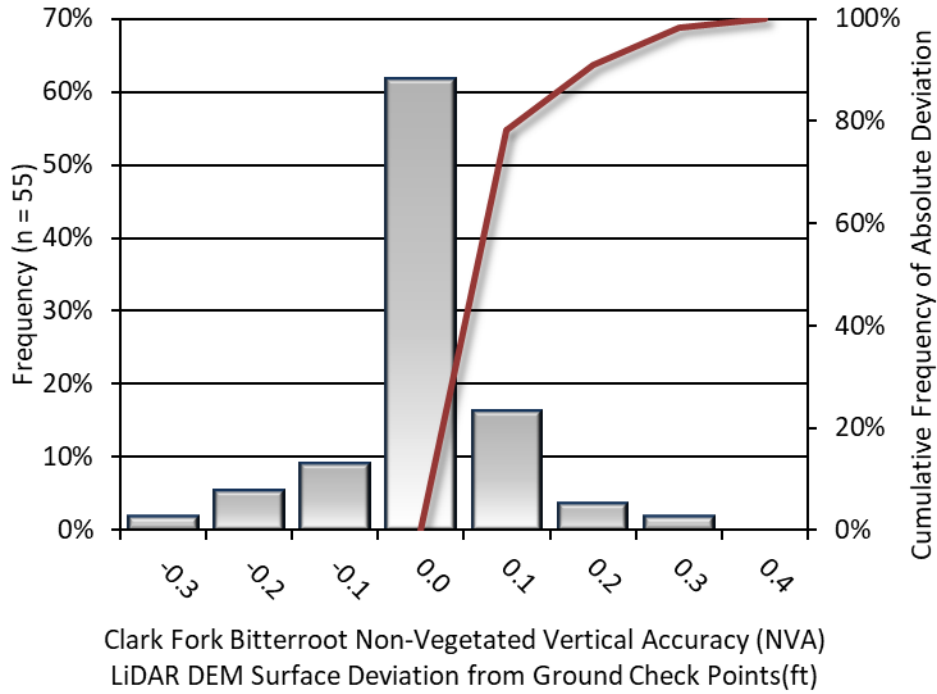


Figure 9: Frequency histogram for LiDAR bare earth DEM surface deviation from ground check point values (NVA)

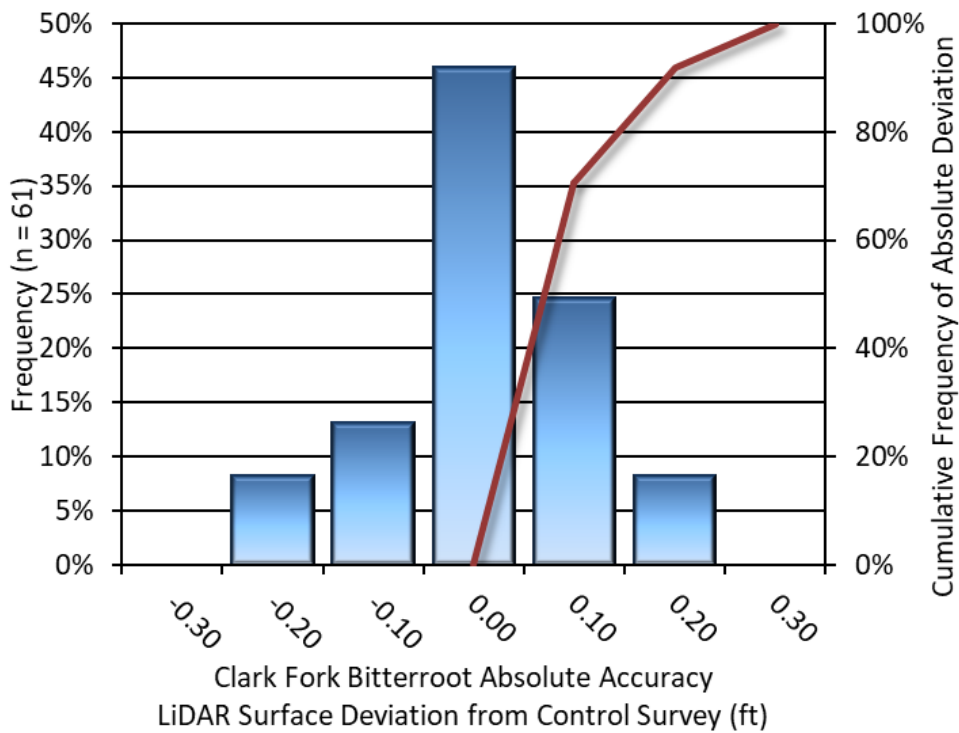


Figure 10: Frequency histogram for LiDAR surface deviation from ground control point values

LiDAR Vegetated Vertical Accuracies

QSI also assessed vertical accuracy using Vegetated Vertical Accuracy (VVA) reporting. VVA compares known ground check point data collected over vegetated surfaces using land class descriptions to the triangulated ground surface generated by the ground classified LiDAR points. For the Clark Fork Bitterroot, Montana survey, 51 vegetated check points were collected, with resulting vegetated vertical accuracy of 0.589 feet (0.180 meters) as compared to the bare earth DEM, evaluated at the 95th percentile (Table 13, Figure 11).

Table 13: Vegetated vertical accuracy results

Vegetated Vertical Accuracy	
Sample	51 points
95 th Percentile	0.589 ft 0.180 m
Average	0.181 ft 0.055 m
Median	0.148 ft 0.045 m
RMSE	0.272 ft 0.083 m
Standard Deviation (1 σ)	0.205 ft 0.062 m

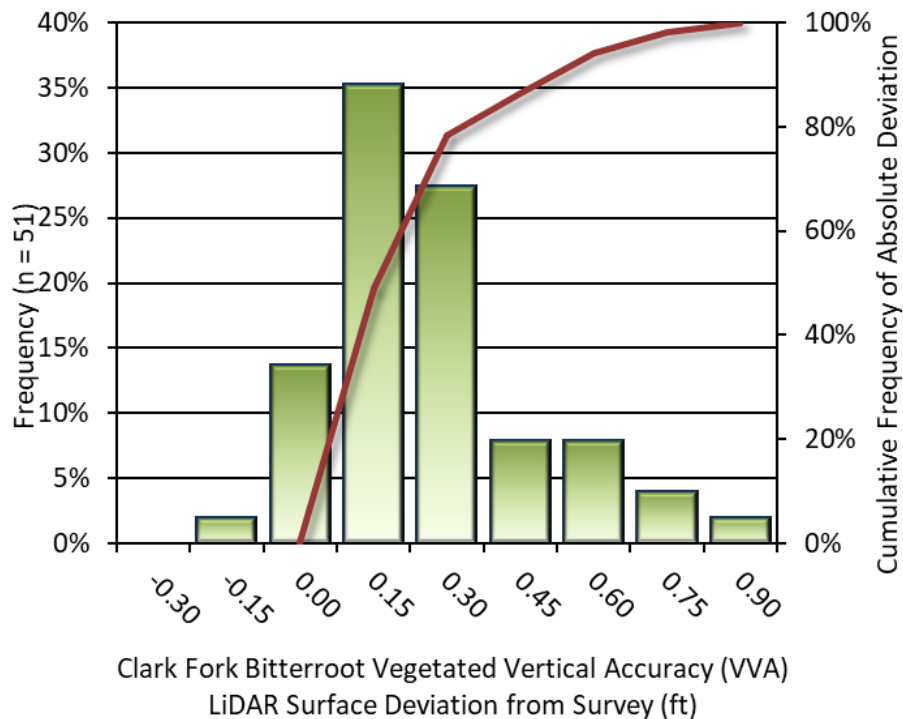


Figure 11: Frequency histogram for LiDAR surface deviation from vegetated check point values (VVA)

LiDAR Relative Vertical Accuracy

Relative vertical accuracy refers to the internal consistency of the data set as a whole: the ability to place an object in the same location given multiple flight lines, GPS conditions, and aircraft attitudes. When the LiDAR system is well calibrated, the swath-to-swath vertical divergence is low (<0.10 meters). The relative vertical accuracy was computed by comparing the ground surface model of each individual flight line with its neighbors in overlapping regions. The average (mean) line to line relative vertical accuracy for the Clark Fork Bitterroot, Montana LiDAR project was 0.096 feet (0.029 meters) (Table 14, Figure 12).

Table 14: Relative accuracy results

Relative Accuracy	
Sample	180 flight line surfaces
Average	0.105 ft 0.032 m
Median	0.112 ft 0.034 m
RMSE	0.114 ft 0.035 m
Standard Deviation (1σ)	0.023 ft 0.007 m
1.96 σ	0.044 ft 0.013 m

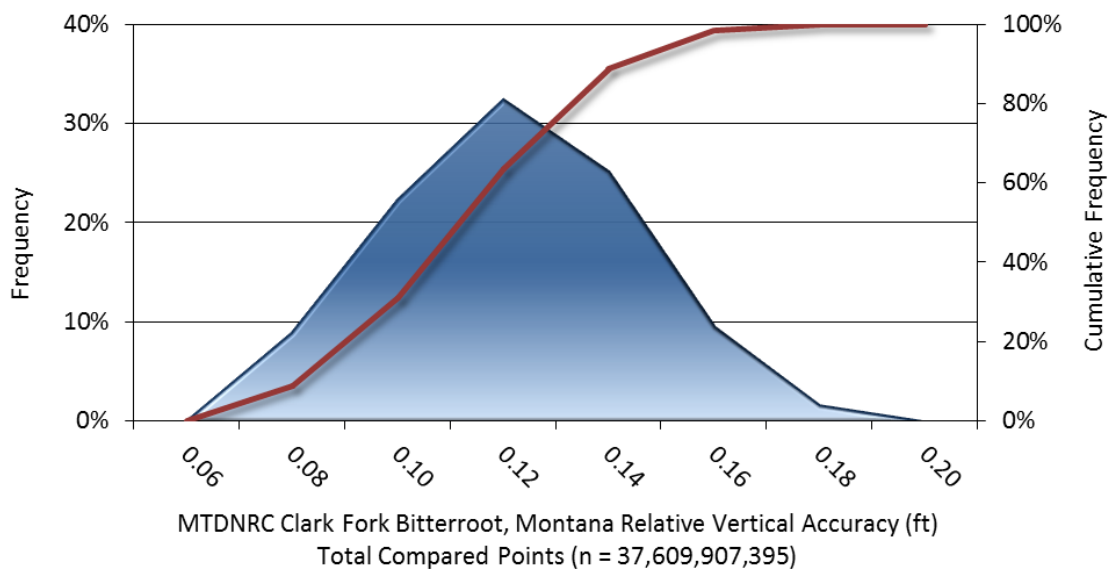


Figure 12: Frequency plot for relative vertical accuracy between flight lines

LiDAR Horizontal Accuracy

LiDAR horizontal accuracy is a function of Global Navigation Satellite System (GNSS) derived positional error, flying altitude, and INS-derived attitude error. The obtained RMSE_r value is multiplied by a conversion factor of 1.7308 to yield the horizontal component (ACC_r) of the National Standards for Spatial Data Accuracy (NSSDA) reporting standard where a theoretical point will fall within the obtained radius 95 percent of the time. Using a flying altitude of 1,800 meters, an IMU error of 0.005 decimal degrees, and a GNSS positional error of 0.015 meters, the horizontal accuracy (ACC_r) for the LiDAR collection is 1.60 feet (0.49 meters) at the 95% confidence level (Table 13). Data from the Jefferson County dataset have been tested to meet horizontal requirements at the 95% confidence level, using NSSDA reporting methods.

Table 15: Horizontal Accuracy

Horizontal Accuracy	
RMSE _r	0.92 ft
	0.28 m
ACC _r	1.60 ft
	0.49 m

CERTIFICATIONS

Quantum Spatial, Inc. provided LiDAR services for the Clark Fork Bitterroot, Montana project as described in this report.

I, Ashley Daigle, have reviewed the attached report for completeness and hereby state that it is a complete and accurate report of this project.

Ashley Daigle
Ashley Daigle (Oct 24, 2019)

Oct 24, 2019

Ashley Daigle
Project Manager
Quantum Spatial, Inc.

I, Steven J. Hyde, PLS, being duly registered as a Professional Land Surveyor in and by the state of Montana, hereby certify that the methodologies, static GNSS occupations used during airborne flights, and ground survey point collection were performed using commonly accepted Standard Practices. Field work conducted for this report was conducted between May 23 and June 16, 2019.

Accuracy statistics shown in the Accuracy Section of this Report have been reviewed by me and found to meet the "National Standard for Spatial Data Accuracy".


Steven J. Hyde



PLS # 60192
Quantum Spatial, Inc..

1-sigma (σ) Absolute Deviation: Value for which the data are within one standard deviation (approximately 68th percentile) of a normally distributed data set.

1.96 * RMSE Absolute Deviation: Value for which the data are within two standard deviations (approximately 95th percentile) of a normally distributed data set, based on the FGDC standards for Non-vegetated Vertical Accuracy (NVA) reporting.

Accuracy: The statistical comparison between known (surveyed) points and laser points. Typically measured as the standard deviation (σ) and root mean square error (RMSE).

Absolute Accuracy: The vertical accuracy of LiDAR data is described as the mean and standard deviation (σ) of divergence of LiDAR point coordinates from ground survey point coordinates. To provide a sense of the model predictive power of the dataset, the root mean square error (RMSE) for vertical accuracy is also provided. These statistics assume the error distributions for x, y and z are normally distributed, and thus we also consider the skew and kurtosis of distributions when evaluating error statistics.

Relative Accuracy: Relative accuracy refers to the internal consistency of the data set; i.e., the ability to place a laser point in the same location over multiple flight lines, GPS conditions and aircraft attitudes. Affected by system attitude offsets, scale and GPS/IMU drift, internal consistency is measured as the divergence between points from different flight lines within an overlapping area. Divergence is most apparent when flight lines are opposing. When the LiDAR system is well calibrated, the line-to-line divergence is low (<10 cm).

Root Mean Square Error (RMSE): A statistic used to approximate the difference between real-world points and the LiDAR points. It is calculated by squaring all the values, then taking the average of the squares and taking the square root of the average.

Data Density: A common measure of LiDAR resolution, measured as points per square meter.

Digital Elevation Model (DEM): File or database made from surveyed points, containing elevation points over a contiguous area. Digital terrain models (DTM) and digital surface models (DSM) are types of DEMs. DTMs consist solely of the bare earth surface (ground points), while DSMs include information about all surfaces, including vegetation and man-made structures.

Intensity Values: The peak power ratio of the laser return to the emitted laser, calculated as a function of surface reflectivity.

Nadir: A single point or locus of points on the surface of the earth directly below a sensor as it progresses along its flight line.

Overlap: The area shared between flight lines, typically measured in percent. 100% overlap is essential to ensure complete coverage and reduce laser shadows.

Pulse Rate (PR): The rate at which laser pulses are emitted from the sensor; typically measured in thousands of pulses per second (kHz).

Pulse Returns: For every laser pulse emitted, the number of wave forms (i.e., echoes) reflected back to the sensor. Portions of the wave form that return first are the highest element in multi-tiered surfaces such as vegetation. Portions of the wave form that return last are the lowest element in multi-tiered surfaces.

Real-Time Kinematic (RTK) Survey: A type of surveying conducted with a GPS base station deployed over a known monument with a radio connection to a GPS rover. Both the base station and rover receive differential GPS data and the baseline correction is solved between the two. This type of ground survey is accurate to 1.5 cm or less.

Post-Processed Kinematic (PPK) Survey: GPS surveying is conducted with a GPS rover collecting concurrently with a GPS base station set up over a known monument. Differential corrections and precisions for the GNSS baselines are computed and applied after the fact during processing. This type of ground survey is accurate to 1.5 cm or less.

Scan Angle: The angle from nadir to the edge of the scan, measured in degrees. Laser point accuracy typically decreases as scan angles increase.

Native LiDAR Density: The number of pulses emitted by the LiDAR system, commonly expressed as pulses per square meter.

APPENDIX A - ACCURACY CONTROLS

Relative Accuracy Calibration Methodology:

Manual System Calibration: Calibration procedures for each mission require solving geometric relationships that relate measured swath-to-swath deviations to misalignments of system attitude parameters. Corrected scale, pitch, roll and heading offsets were calculated and applied to resolve misalignments. The raw divergence between lines was computed after the manual calibration was completed and reported for each survey area.

Automated Attitude Calibration: All data were tested and calibrated using TerraMatch automated sampling routines. Ground points were classified for each individual flight line and used for line-to-line testing. System misalignment offsets (pitch, roll and heading) and scale were solved for each individual mission and applied to respective mission datasets. The data from each mission were then blended when imported together to form the entire area of interest.

Automated Z Calibration: Ground points per line were used to calculate the vertical divergence between lines caused by vertical GPS drift. Automated Z calibration was the final step employed for relative accuracy calibration.

LiDAR accuracy error sources and solutions:

Type of Error	Source	Post Processing Solution
GPS (Static/Kinematic)	Long Base Lines	None
	Poor Satellite Constellation	None
	Poor Antenna Visibility	Reduce Visibility Mask
Relative Accuracy	Poor System Calibration	Recalibrate IMU and sensor offsets/settings
	Inaccurate System	None
Laser Noise	Poor Laser Timing	None
	Poor Laser Reception	None
	Poor Laser Power	None
	Irregular Laser Shape	None

Operational measures taken to improve relative accuracy:

Low Flight Altitude: Terrain following was employed to maintain a constant above ground level (AGL). Laser horizontal errors are a function of flight altitude above ground (about 1/3000th AGL flight altitude).

Focus Laser Power at narrow beam footprint: A laser return must be received by the system above a power threshold to accurately record a measurement. The strength of the laser return (i.e., intensity) is a function of laser emission power, laser footprint, flight altitude and the reflectivity of the target. While surface reflectivity cannot be controlled, laser power can be increased and low flight altitudes can be maintained.

Reduced Scan Angle: Edge-of-scan data can become inaccurate. The scan angle was reduced to a maximum of $\pm 30^\circ$ from nadir, creating a narrow swath width and greatly reducing laser shadows from trees and buildings.

Quality GPS: Flights took place during optimal GPS conditions (e.g., 6 or more satellites and PDOP [Position Dilution of Precision] less than 3.0). Before each flight, the PDOP was determined for the survey day. During all flight times, a dual frequency DGPS base station recording at 1 second epochs was utilized and a maximum baseline length between the aircraft and the control points was less than 13 nm at all times.

Ground Survey: Ground survey point accuracy (<1.5 cm RMSE) occurs during optimal PDOP ranges and targets a minimal baseline distance of 4 miles between GPS rover and base. Robust statistics are, in part, a function of sample size (n) and distribution. Ground survey points are distributed to the extent possible throughout multiple flight lines and across the survey area.

50% Side-Lap (100% Overlap): Overlapping areas are optimized for relative accuracy testing. Laser shadowing is minimized to help increase target acquisition from multiple scan angles. Ideally, with a 50% side-lap, the nadir portion of one flight line coincides with the swath edge portion of overlapping flight lines. A minimum of 50% side-lap with terrain-followed acquisition prevents data gaps.

Opposing Flight Lines: All overlapping flight lines have opposing directions. Pitch, roll and heading errors are amplified by a factor of two relative to the adjacent flight line(s), making misalignments easier to detect and resolve.